THERMAL CONTRACTION CRACK POLYGONS ON MARS: CLASSIFICATION, DISTRIBUTION, AND CONTEXT FOR PHOENIX FROM NORTH AND SOUTH POLAR HIRISE OBSERVATIONS. J. S. Levy[1], J. W. Head[1], D. R. Marchant[2], [1]Brown Univ. Dept. of Geological Sciences, Providence, RI, 02906. [2]Boston Univ. Dept. of Earth Sciences, Boston, MA, 02215. joseph_levy@brown.edu.

Introduction: The detection of subsurface ice at the polygonally-patterned Phoenix landing site [1] is the culmination of over thirty years of Mars permafrost and polygons research [2-6]. The exploration of martian polygonally patterned ground addresses several critical questions related to recent martian habitability and climate processes: 1) what is the origin of ice in the shallow martian subsurface (e.g., cyclical vapor diffusion or primary deposition of now-buried ice sheets) [7-11]; 2) to what extent is liquid water involved in martian polygon development [5]; does thermal contraction cracking account for the complete range of polygonally patterned ground observed on Mars [5]; do the ages of different polygonally patterned units vary systematically [5, 8]; and how does polygonally patterned ground fit into broader-scale ice-related activity during the late Amazonian [7, 9, 12]?

Polygon classification in terrestrial polar environments is based on morphology, structure, and origin processes. On Earth, thermal contraction crack polygons can be divided into three types: ice-wedge, sand-wedge, and sublimation polygons; each of which forms under a unique set of climate and substrate-composition conditions [13, 14]. Although the thermal contraction cracking process under martian conditions is well understood [15], classification systems for polygonally patterned ground on Mars have until now relied primarily on imaging data at resolutions comparable to the scale of the polygons of interest [5]. Here, we classify small polygons (<25 m diameter) visible in HiRISE images into seven morphological groups distinguishable by characteristic surface morphologies. This morphological classification can provide the basis for further analysis of polygon evolution processes [16].

Survey Parameters: We present a survey of 823 full-resolution HiRISE images of martian polar regions (30-80°N), spanning primary science phase orbits 001331 to 006981 [17]. Of the surveyed images, 483 contain polygonally patterned ground (59%), with polygon frequency higher at higher latitudes.

Polygon Classification and Distribution: We divide polygons into 7 morphological varieties (Fig. 1). Commonly more than one variety is present in a single HiRISE image, suggesting variability in polygon-forming substrate conditions on 100 m to km length scales [18]. Polygon groups are latitude-dependent, suggesting a climatic control on polygon morphology.

High Relief (HR). High relief polygons have strong topographic contrasts between polygon interiors and topographically-depressed, straight-sided polygon troughs. HR are morphologically similar to S1 terrain described by [5], with diameters averaging 6.1 m in the northern hemisphere, and 5.6 in the southern hemisphere. In places, well-developed HR polygons fringe central clusters of HR polygons with smaller and less-well defined troughs.

Flat-Top Small (FTS). Flat-top small polygons are the predominant northern hemisphere polygon class (present in 119 images) and represent a significant population in the southern hemisphere (present in 48 images). FTS polygons are all broadly similar to the S group described by [5]. FTS were first described in proximity to the NASA Phoenix landing site [16, 19-21]. FTS are straight-sided polygons (mean diameter 5.2 m in the northern hemisphere, 10.1 m in the southern hemisphere) with visible, negative trough relief. FTS trough intersections are commonly both near-orthogonal and near-hexagonal, outlining relatively flat-topped, high-center polygons. FTS polygon troughs form sharply-defined networks of fractures. Frost seasonally accumulates in FTS troughs, and may be preserved into the spring season. Boulder piles are present overlying approximately 40% of northern hemisphere FTS polygons, forming "basketball terrain" light and dark patterns observed in MOC images [4, 21]. Basketball terrain caused by boulder piles is absent in southern hemisphere images analyzed in this survey. Patterned mantle material overprints all craters analyzed (Fig. 2).

Irregular (IRR). Irregular polygons are composed of poorly polygonalized networks of fractures, commonly consisting of long, sinuous cracks (some of which have raised shoulders) and smaller, polygon-forming fractures. IRR trough intersections are commonly near-orthogonal. IRR have a distinctly "wormy" surface texture on account of the longer, through-going fractures. Where well-formed IRR polygons are present, they are commonly flat-topped, with high centers; however, IRR polygons are most commonly outlined by incomplete fracture networks, giving them a degraded appearance. IRR are present in 83 images in the northern hemisphere, including those surrounding the Phoenix lander, and are present in 18 images in the southern hemisphere.

Subdued (SUB). Subdued polygons are bounded by depressed troughs that are broader (up to 1-2 m) and less-straight than those outlining FTS polygons, making them broadly similar to [5] S3 polygons. Subdued polygons average 16 m in diameter in the northern hemisphere and 16.8 m in diameter in the southern hemisphere. SUB polygon troughs are commonly lighter toned than polygon interiors. Subdued polygon interiors are commonly flat, to gently convex up. SUB commonly have small, ~1 m-scale boulders accumulated in inter-polygon troughs, forming networks of lineated boulders. Subdued polygon trough intersections are commonly near-hexagonal. SUB polygons are present in 38 images in the northern hemisphere and are present in 16 images in the southern hemisphere.

Gullygons. "Gullygons" are polygons that are present in gully alcoves, along gully channels, or that interact with gully fans [22, 23]. Gullygons are commonly flat-centered with sharply defined, bounding troughs, forming polygons which average ~11 m in diameter in the northern hemisphere and 9.3 m in diameter in the southern hemisphere. Gullygon trough intersections are commonly near-orthogonal, particularly when gullygons are present on slopes. Stratigraphic relationships within gully-polygon systems indicate that polygon development both precedes and post-dates gully activity in some images containing gullygons [22, 23]. Gullygons are rare in the northern hemisphere, and are present in 25 images; gullygons are common in the southern hemisphere, and are present in 91 images.

Peak-Topped (PT). Peak-top polygons are characterized by steeply peaked or pointed, convex-up polygon interiors. Shadow measurements indicate that PT polygon interiors can be inclined up to ~30°. PT are bounded by shallow, narrow polygon troughs. Peak-top polygons average 9.1 m in diameter in the northern hemisphere and 8.9 m in the southern hemisphere. PT trough intersections are commonly near-orthogonal. PT form in association with mixed-center polygons (below) as well as in isolation. PT are present in 22 images in the northern hemisphere and are present in 13 images in the southern hemisphere.

Mixed-Center (MX). Mixed-center polygons are one of the most pervasive classes of polygons on Mars. MX polygons have two distinct forms which transition into one another over meter length-scales: high-center and low-center. High-center MX polygons are composed of depressed surface troughs that intersect at both near-orthogonal and near-hexagonal intersections, forming polygons with topographically high interiors relative to their boundaries. High-center MX polygon interiors are commonly flat-topped to slightly convex-up. Low-center MX polygons are composed of troughs with raised shoulders that intersect at near-orthogonal and near-hexagonal intersections, forming polygons with depressed centers, relative to the raised rims. Low-center MX polygons have smooth, flat, depressed interiors. Low-center MX polygons occur predominantly on steep-walled, scalloped depressions and on mantled slopes adjacent to "brain terrain" surfaces [24, 25]. MX polygon diameter is approximately constant between high- and low-center forms, averaging 11.3 m in the northern hemisphere and 9.9 m in the southern hemisphere. MX polygons are present in 57 northern hemisphere images and in 76 images in the southern hemisphere. Polygons similar to the MX group have been identified in and around the enigmatic scallops in Utopia Planitia, and in circum-Hellas and Argyre terrains [26-30], as well as in latitude-dependent mantle deposits overlying lineated valley fill and concentric crater fill [24, 25].

Conclusions: Polygons analyzed in this survey are present primarily in surface units which mantle underlying topography (e.g., the martian latitude-dependent mantle). All observed polygon classes, with the exception of gullygons, can be interpreted to result from a range of cold-desert geomorphic processes that do not require the presence of liquid water [31]. Crater counts indicate that polygonally patterned units in the northern hemisphere are found to follow a strong correlation between latitude and age. Equator-ward polygonally patterned units, such as mixed-center polygons are the oldest (~1.3 Ma), followed by intermediate polygonally patterned units (e.g., subdued polygons, at ~130 ka). Finally, high-latitude northern plains polygons (e.g., FTS) are found to be the youngest (~50-100 ka). Differences in polygon surface expression can be used as an aid in understanding how recent, ice-rich mantling units have been deposited across a variety of martian latitudes and microclimate zones—a critical step in assessing the changing habitability of martian permafrost environments.

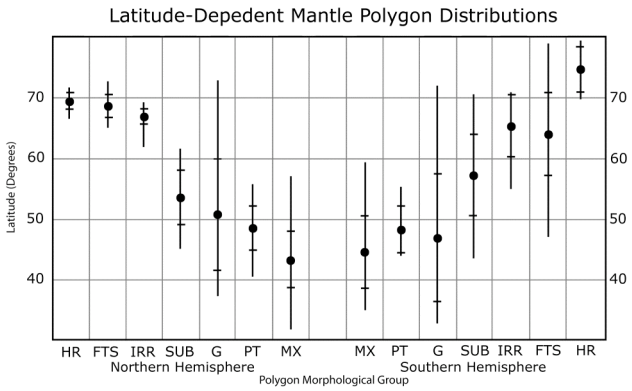

Figure 1. Global distribution of small martian thermal contraction crack polygon morphological groups. For each class we plot mean latitude of occurrence (bold circle), the range of occurrence (vertical bars) and the latitudes which bracket one standard deviation of the range of occurrence (horizontal cross-bars). Polygon morphological group is a strong function of latitude, and is largely symmetrical across north and south hemispheres, suggesting global-scale climate controls on polygon morphology.

References: [1] Smith, P.H. & Team (2008) *AGU Fall Mtg.*, Abstr. #P13F-01. [2] Lucchitta, B.K. [1981] *Icarus*, *45*, 264-303. [3] Mutch, T.A., et al. (1976) *Science*, *194*, 1277-1283. [4] Malin, M.C. & Edgett, K. S. (2001) *JGR, 106*, 23,429-23,540. [5] Mangold, N. (2005) *Icarus*, *174*, 336-359. [6] Mangold, N., et al. (2004) *JGR, 109*, doi:10.1029/2004 JE002235. [7] Head, J.W., et al. (2003) *Nature*, *426*, 797-802. [8] Kostama, V.-P., et al. (2006) *GRL, 33*, doi:10.1029/ 2006GL025946. [9] Mustard, J.F., et al. (2001) *Nature, 412,* 411-414. [10] Schorghofer, N. (2007) *Nature*, *449,* 192-194. [11] Schorghofer, N. & Aharonson, O. (2005) *JGR, 110,* doi: 10.1029/2004JE002350. [12] Milliken, R.E., et al. (2005) *JGR, 108*, doi:10.1029/2002JE002005. [13] Black, R.F. (1976) *Quat. Res., 6*, 3-26. [14] Marchant, D.R. & Head, J. W. (2007) *Icarus, 192*, 187-222. [15] Mellon, M.T. (1997) *JGR, 102,* 25,617-25,628. [16] Levy, J.S., et al. (2008) *GRL, 35,* doi:10.1029/ 2007GL032813. [17] McEwen, A.S., et al. (2007) *JGR, 112,* doi: 10.129/ 2005JE002605. [18] Bandfield, J.L. (2007) *Nature, 447*, 64-67. [19] Arvidson, R., et al. (2008) *JGR, 113*, doi:10.1029/2007JE003021. [20] Mellon, M.T., et al. (2008) *JGR, 113*, doi:10.1029/2007JE003039. [21] Mellon, M.T., et al. (2007) *7th* Mars, Abstr. #3285. [22] Levy, J.S., et al. (2008) *Ant. Sci., 20,* doi:10.1017/ S0954102008001375. [23] Levy, J.S., et al. (2008) *Icarus, In Press.* [24] Dobrea, E.Z.N., et al. (2007) *7th Mars,* Abstr #3358 [25] Levy, J.S., et al. (2009) *JGR, In Press.* [26] Costard, F., et al. (2008) *LPSC39*, Abstr. #1274. [27] Lefort, A., et al. (2007) *LPSC38,* Abstr. #1796. [28] Morgenstern, A., et al. (2007) *JGR, 112*, doi: 10.1029/2006JE002869. [29] Soare, R.J. (2008) *EPSL, 272,* 382-393. [30] Zanetti, M., et al. (2008) *LPSC39,* Abstr. #1682. [31] Levy, J.S., et al. (2009) *JGR, In Press.*

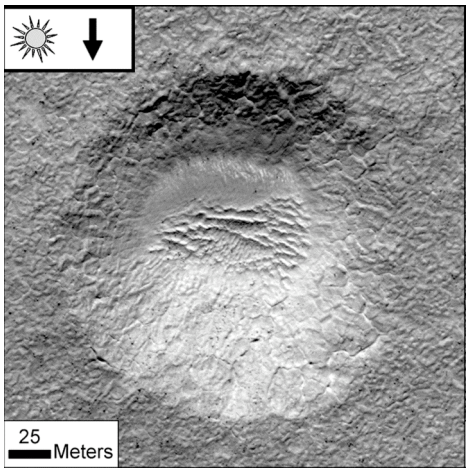

Figure 2. Example impact crater modified by polygon-forming processes and mantle deposition.